nature
structural biology

An asymmetric NFAT1 dimer on a pseudo-palindromic κB-like DNA site

Lei Jin[1,5], Piotr Sliz[1,5], Lin Chen[1,3], Fernando Macián[2,4], Anjana Rao[2], Patrick G Hogan[2] & Stephen C Harrison[1]

The crystal structure of the NFAT1 Rel homology region (RHR) bound to a pseudo-palindromic DNA site reveals an asymmetric dimer interaction between the RHR-C domains, unrelated to the contact seen in Rel dimers such as NFκB. Binding studies with a form of the NFAT1 RHR defective in the dimer contact show loss of cooperativity and demonstrate that the same interaction is present in solution. The structure we have determined may correspond to a functional NFAT binding mode at palindromic sites of genes induced during the anergic response to weak TCR signaling.

Members of the NFAT family of transcription factors contain a module of ~300 residues known as a Rel homology region (RHR)[1–3]. As originally characterized in proteins of the Rel family (such as the proto-oncogene product c-Rel and the components of NFκB), the RHR has two Ig-like domains, RHR-N and RHR-C, linked by a short hinge (**Fig. 1a**). Rel family members form homo- and heterodimers that bind sites on DNA with partial palindromic character. A critical element in each half site is a GG sequence, and the center of the site is generally AT-rich. DNA contacts and base-pair recognition are largely functions of the RHR N-terminal domain (RHR-N); dimerization is a principal function of the RHR C-terminal domain (RHR-C). In their 'classic' binding mode, NFAT family members do not dimerize with themselves or with each other; rather, they cooperate with AP-1, the heterodimer of Fos and Jun family members, to recognize a composite site (**Fig. 1b**). The structure of the NFAT1 RHR, bound with the DNA-binding segment of a Fos-Jun heterodimer to the ARRE2 site from the interleukin-2 (IL-2) promoter, showed that most of the NFAT–AP-1 contacts are DNA proximal and that the RHR-C makes at best a modest interaction with Fos[4]. The surface on NFAT1 RHR-C homologous to the dimerization face of RHR-Cs from Rel-family members, although moderately hydrophobic and remarkably similar to the corresponding surface on NFκB components, faces solvent and does not participate in any intermolecular contact.

What, then, is the role of the NFAT RHR-C? It is unlikely to be merely a passenger of evolutionary re-use, as other transcription factors with Ig-like DNA-binding domains (such as p53) dispense with a second Ig-like fold. Moreover, there are regulatory sites that respond to NFAT activation but that do not contain the classic composite sequence of the ARRE2 (a GGA core followed five base pairs downstream by an often rather divergent AP-1 site). Rather, they contain a κB-like sequence, GGAGGAXXXTCCTCC. Such sequences bind two NFAT1 subunits with measurable cooperativity[5]. In view of its close structural relationship with Rel-family proteins, one might reasonably have supposed that NFAT1 would form a Rel-like dimer on such sites and that the conserved RHR-C structures would generate a conserved dimer interaction.

To explore a potential dimer interaction, we have crystallized the NFAT1 RHR bound to a pseudo-palindromic site derived from the human IL-8 promoter. The structure, determined to a resolution of 3.1 Å and reported here, indeed shows a dimer of NFAT, but with an asymmetric interaction between RHR-C domains rather than a Rel-like geometry. Neither of the surfaces of the RHR-C that participate in this asymmetric dimer contact is the one that mediates dimerization in NFκB. Moreover, the asymmetrically paired RHR-C domains are flexibly linked to their more symmetrically disposed, DNA-bound, RHR-N counterparts. We have tested the functional consequences of the observed dimer interaction by generating a deletion mutation in the cc′ loop (614–621) and measuring its effect on dimer binding. We conclude that the asymmetric structure seen in the crystals corresponds to a functional dimer. The same asymmetric contact appears in the structure of NFAT1 bound to a κB-like site from the HIV-1 LTR (see accompanying paper by Giffin *et al.*[6]). In lymphocytes, NFAT family members have been shown to activate two classes of genes: those with composite NFAT–AP-1 sites that are induced during a productive immune response, and a much smaller number of genes that do not depend on NFAT–AP-1 cooperation and are associated with an 'anergic' response. We propose that the asymmetric dimer interaction detected crystallographically may represent the state of NFAT protein on these AP-1-independent regulatory regions.

[1]Department of Biological Chemistry and Molecular Pharmacology and Howard Hughes Medical Institute, Harvard Medical School, Boston, Massachusetts 02115, USA. [2]Center for Blood Research, Department of Pathology, Harvard Medical School, 200 Longwood Avenue, Boston, Massachusetts 02215, USA. [3]Present address: Department of Chemistry and Biochemistry, University of Colorado at Boulder, Boulder, Colorado 80309, USA. [4]Present address: Department of Pathology, 1300 Morris Park Avenue, Albert Einstein College of Medicine, Bronx, New York 10461, USA. [5]These authors contributed equally to this work. Correspondence should be addressed to S.C.H. (harrison@crystal.harvard.edu).

Published online 31 August 2003; doi:10.1038/nsb975

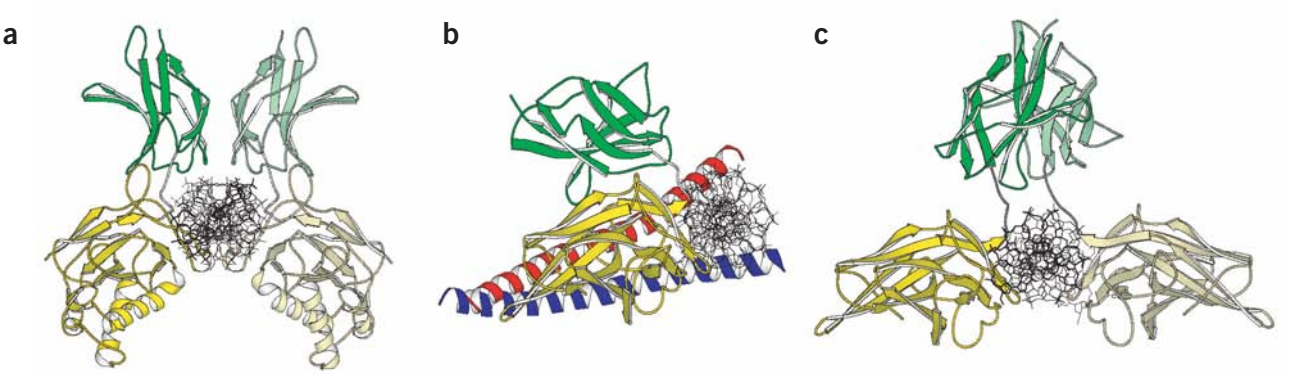

Figure 1 Structures of members of the RHR family of transcription factors bound to DNA. (**a**–**c**) Views along the DNA axis of (**a**) the p50 homodimer of NFκB on a κB site (**b**) the NFAT1–RHR–Fos-Jun ternary complex on the ARRE2 site and (**c**) one of the NFAT1 dimers from the present crystal structure. The RHR-N domain is yellow and its symmetry mate light yellow; the RHR-C domain is green and its partner light green; Fos, red; Jun, blue. Colors here are used throughout the rest of the figures.

RESULTS

Borrowing from the 'butterfly' description for the NFκB–DNA complex[7–9] (**Fig. 1a**), we can characterize the dimeric NFAT1–DNA complex as a 'butterfly with a twist' (**Fig. 1c**). The NFAT1 RHR binds, as anticipated, with its RHR-N in contact with DNA, much as in the NFAT1–Fos-Jun–ARRE2 complex or in the various NFκB–DNA complexes so far analyzed. Contrary to expectations, however, the dimer contacts between the RHR-C domains do not at all resemble those in NFκB (**Fig. 1**). The interaction is completely asymmetric. Two quite different surfaces are in contact, and neither is the homolog of the surface found at the symmetric interface in NFκB.

The disordered linker between RHR-N and RHR-C is extended so that the paired RHR-C domains have only tenuous contacts with DNA backbone and none with RHR-N. Indeed, the orientation and position of the RHR-C dimer module with respect to the rest of the complex is quite different for each of the three complexes in the crystallographic asymmetric unit (**Fig. 2**), and the asymmetry of the paired RHR-C domains is not correlated with the orientation of the DNA site to which the dimer binds. Thus, the disordered linker tethers the dimer module quite flexibly to the rest of the structure. Owing to the asymmetric nature of the RHR-C domains, there should be two NFAT1-RHR–DNA conformers co-existing with equal probability in solution. Both of the conformers have been observed in the orthorhombic crystal form as a result of the unique crystal packing. Despite totally different crystallographic environments, however, all three pairs of RHR-C domains have essentially identical asymmetric dimer contacts. The dimer interface we see is therefore independent of the crystallographic environment, reinforcing our conviction that it represents an interaction that also occurs in solution.

DNA recognition

The DNA fragments stack end-to-end in the crystal, creating an approximate non-crystallographic three-fold screw axis (**Fig. 2a**). Each segment is somewhat bent and tilted with respect to the *c*-axis, creating a slightly superhelical stack. Contacts between the RHR-N and DNA are essentially the same as those seen in the NFAT1–Fos-Jun–ARRE2 complex[4] (see also accompanying paper[6]). The loop between strands A and B, the 'recognition loop' in all RHR proteins,

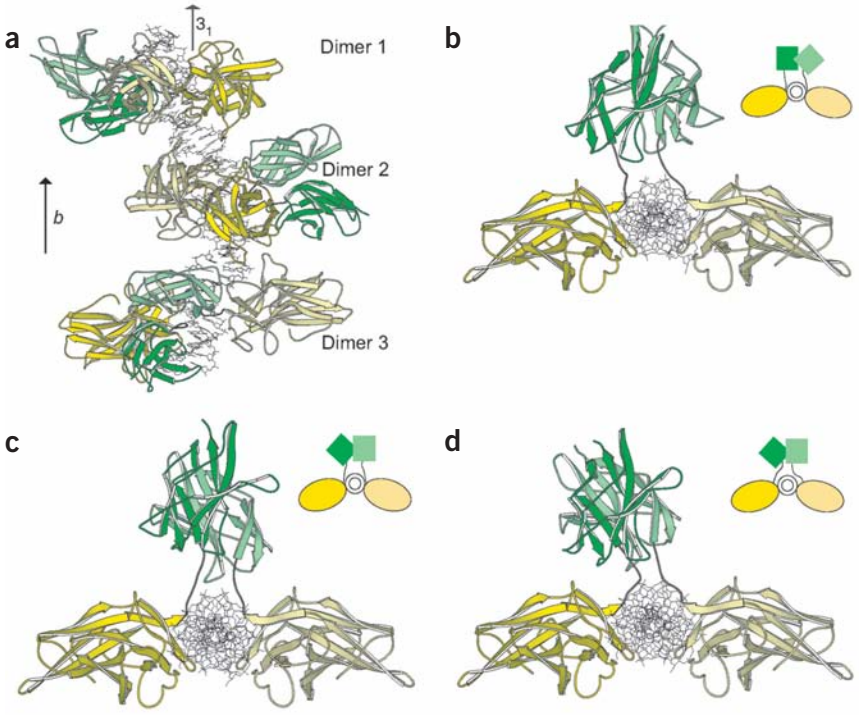

Figure 2 View of the three crystallographically nonequivalent dimers in the orthorhombic crystal form of the NFAT1 dimer–DNA complex. (**a**) One asymmetric unit of the $P2_12_12_1$ crystal, with the non-crystallographic three-fold screw axis shown. The view is normal to the DNA axis. (**b**–**d**) Each of the three crystallographically distinct dimers, viewed along the DNA axis, with the RHR-N domains in corresponding orientations. The inset diagrams show the asymmetry of the RHR-C interactions. The orientation of the asymmetric RHR-C pair in **b** is opposite from those in **c** and **d**. The tilt of the RHR-C dimer axis varies among the dimers by up to 10°.

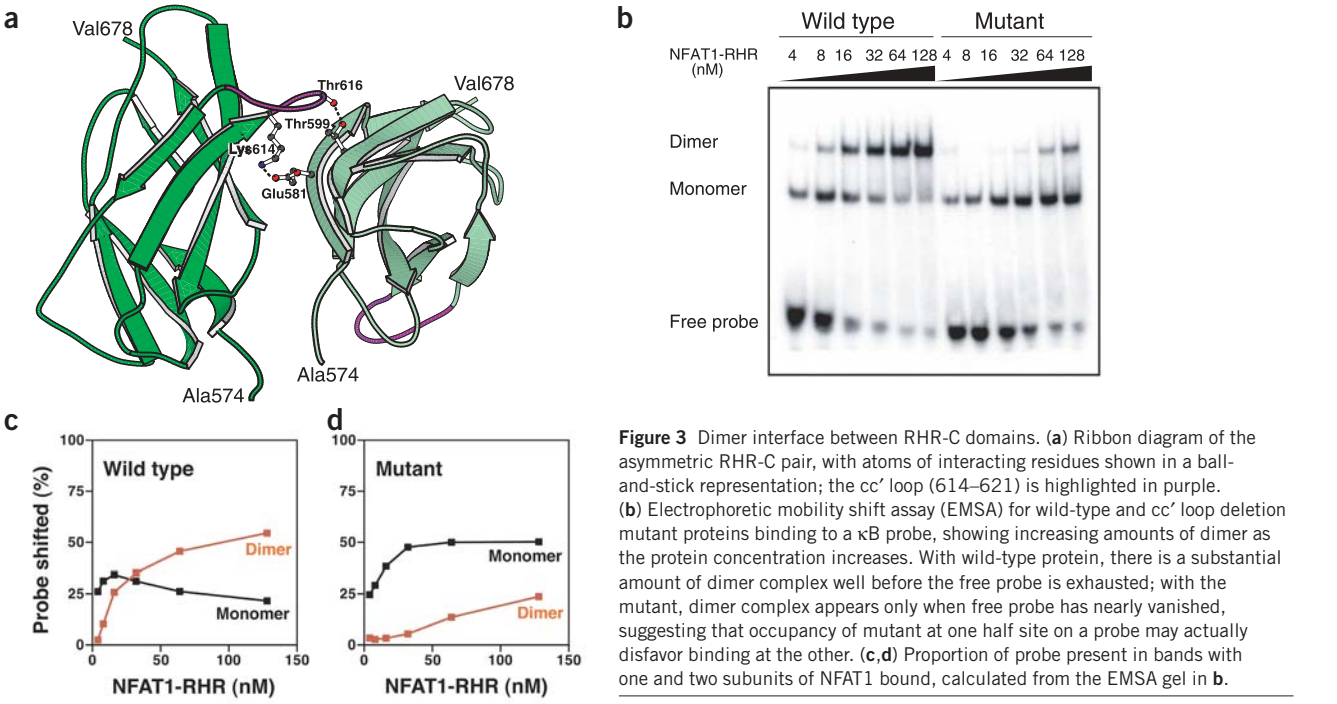

Figure 3 Dimer interface between RHR-C domains. (**a**) Ribbon diagram of the asymmetric RHR-C pair, with atoms of interacting residues shown in a ball-and-stick representation; the cc′ loop (614–621) is highlighted in purple. (**b**) Electrophoretic mobility shift assay (EMSA) for wild-type and cc′ loop deletion mutant proteins binding to a κB probe, showing increasing amounts of dimer as the protein concentration increases. With wild-type protein, there is a substantial amount of dimer complex well before the free probe is exhausted; with the mutant, dimer complex appears only when free probe has nearly vanished, suggesting that occupancy of mutant at one half site on a probe may actually disfavor binding at the other. (**c**,**d**) Proportion of probe present in bands with one and two subunits of NFAT1 bound, calculated from the EMSA gel in **b**.

inserts into the major groove. Specification of the NFAT consensus recognition motif, GGA, is just as in the NFAT1–Fos-Jun–ARRE2 complex: Arg421 and Arg430 contact the guanines, and Gln571 the adenine. The interactions are classic Seeman-Rich bidentate hydrogen-bond patterns[10]. Tyr424 contacts the methyl group of the thymine base-paired with the consensus adenine, further contributing to specificity at this position.

A key set of DNA backbone contacts include those at the base of the E′F loop (528–540), which contacts Jun in the NFAT1–Fos-Jun–ARRE2 quaternary complex[4]. This loop is fully ordered in the present structure, despite the absence of AP-1. Moreover, the way each NFAT monomer encounters its DNA half site is identical to the way it does so in the NFAT1–Fos-Jun–ARRE2 complex. This comparison shows that there is no reorientation of the NFAT1 RHR-N on DNA induced by adjacency of AP-1, as has been suggested from an NMR structure of an RHR-N–DNA complex from NFAT2 (ref. 11).

Asymmetric dimer interactions

At the dimer interface (**Fig 3a**), the cc′ loop of one partner wraps across the ab surface of the other. A network of polar interactions connects the two subunits. The total buried surface at this contact is modest (~1,500 Å^2), and we believe that it is unlikely to hold the dimer together in the absence of a common DNA substrate. That is, free NFAT1 is likely to be monomeric under all conditions, but binding to suitable, roughly palindromic DNA sites will be enhanced through the cooperativity introduced by the dimer contact. We observe that most of the residues participating directly in the contact are invariant among NFATs 1–4.

Effect of loop mutations

We have confirmed the relevance of the asymmetric dimer to NFAT1 DNA binding in solution by studying the effects of a deletion mutation designed to destabilize the observed contact (**Fig. 3b–d**). The wild-type protein binds with modest cooperativity to a pseudo-palindromic DNA site derived from the IL-8 promoter. Deletion of the cc′ loop, by replacing residues 614–621 with Ser-Gly, weakens binding of NFAT1 dimers, but not binding of monomers. We thus believe that the dimer bound to DNA in solution indeed has the asymmetric structure of the dimer seen bound to DNA in the crystals. The loop deletion does not compromise binding to an ARRE2 site (data not shown). There is a comparable decrease in dimer formation by wild-type NFAT1 when five additional base pairs are introduced into the IL-8 promoter oligonucleotide between the two GGA half sites, moving one of the binding positions to the opposite face of the DNA duplex (data not shown).

DISCUSSION

NFAT dimers on other DNA sites

The NFAT and NFκB families are clearly branches of a larger, Rel-homology kinship. Known physiological NFκB–DNA complexes contain homo- or heterodimers that recognize a site with core elements of two G-C base pairs (G-C/G-C) that are related by two-fold symmetry and separated by five intervening nucleotides. The site from the IL-8 promoter that we have studied here has such a κB-like consensus, and the two RHR-N domains dock against it rather like two RHR-N domains from an NFκB dimer. This docking is the same in the two crystal forms we have studied. The asymmetric dimer linkage through RHR-C is quite unlike any NFκB interaction, however.

Two other NFAT-family dimer structures have been determined. One, that of NFAT5 (also known as TonEBP) on an asymmetric site from the promoter of the human sodium/myoinositol cotransporter gene, shows a NFκB-like dimer, with essentially symmetrical RHR-C contacts, bound to a G-C/G-C element on one side, a nonconsensus C-G/T-A element on the other, and six intervening nucleotides[12]. Because of the additional base pair intervening between the core half sites (a 'stretched' binding mode), the two RHR-N domains approach each other more closely around the 'rear' of the DNA than in the complex described here. As a result, there are two-fold con-

Table 1 Data collection and refinement statistics

	Trigonal	Orthorhombic
Data collection		
Space group	$P3_121$	$P2_12_12_1$
Cell parameters (Å)		
a	144.4	81.7
b	144.4	122.9
c	127.3	241.6
Resolution (Å)[a]	30–3.9 (4.1–3.9)	30–3.1 (3.2–3.1)
Mosaicity	0.35	0.50
Total reflections[a]	53,331 (7,604)	124,267 (9,841)
Unique reflections[a]	14,224 (2,019)	37,145 (4,269)
Completeness (%)[a]	99.9 (99.8)	82.4 (77.0)
R_{sym} (%)[a,b]	12.5 (29.1)	9.5 (30.8)
$I / \sigma I$[a]	9.4 (3.9)	9.0 (2.7)
Refinement statistics		
R_{work}[b]	N/A	29.6
R_{free}[b]	N/A	31.9
R.m.s. deviation from ideal		
Bonds (Å)	N/A	0.01
Angles (°)	N/A	1.5

[a]Values in parentheses are for the highest-resolution shell. [b]$R_{sym} = \Sigma|(I_{hkl} - I_{<hkl>})| / (\Sigma I_{hkl})$, where $I_{<hkl>}$ is the mean intensity of all reflections equivalent to reflection *hkl* by symmetry; R_{work} (R_{free}) $= \Sigma||F_o| - |F_c|| / \Sigma|F_o|$; 5% of data were used for R_{free}. N/A, not applicable.

tacts between the short helices in the E′F loops—the same loops that mediate the most critical contact with the Fos-Jun heterodimer in the quaternary complex with ARRE2. This additional interaction allows the NFAT5 dimer to encircle fully the DNA double helix. A second NFAT-family dimer complex is described in the accompanying paper[6]: it is NFAT1 with a site on which it can recognize G-C/G-C elements separated by six rather than five base pairs. As expected from the half-site spacing and from the NFAT5 structure just described, the encirclement contact of E′F loops is also present in the stretched NFAT1 complex. Indeed, the site in that complex has three G-C base pairs in one of its half sites, and NFAT1 can 'choose' to bind with five or six base pairs intervening between the two similarly recognized G-C/G-C elements. The E′F dimer contact probably dictates the latter choice. The RHR-C interaction is in any case identical to the asymmetric dimer described here, providing further evidence for the relevance of the asymmetric interface. NFκB p50 homo-dimers can also bind sites with six base pairs between the two G-C/G-C core elements[7], but the short E′F loop does not make an encircling dimer contact.

NFAT dimers in functional promoters

The plasticity of DNA-recognition geometries for NFAT-family members evidently corresponds to their participation in a variety of distinct regulatory pathways, depending on different partner proteins. In lymphocytes, at least two classes of genes respond to NFAT family members[13]. In the 'classic' response, triggered by strong antigen-receptor stimulation and full costimulation (for example, from CD28), NFAT cooperates with AP-1 and other transcription factors at sites such as the IL-2 promoter. Loci in this category appear to contain composite binding elements for NFAT and AP-1 (ref. 2). In the 'anergic' response, triggered by weaker antigen receptor stimulation and no costimulatory signal, NFAT acts independently of AP-1 and NFκB[13]. The structure described here might correspond to a functional NFAT binding mode at these sites.

METHODS

Preparation of NFAT1-RHR dimer–DNA complex. His-tagged human NFAT1-RHR (residues 396–678) was expressed in *Escherichia coli*, purified as described previously[4], and concentrated to 1.6 mM in 10 mM HEPES, pH 7.5, 1 mM DTT, 100 mM NaCl, 20% (v/v) glycerol and 500 mM ammonium acetate.

The double-stranded DNA used for crystallization has the sequence

5′-TTGAGGAATTTCCA-3′
3′-CTCCTTAAAGGTAA-5′

The underlined sequence is present in the human IL-8 promoter. The oligonucleotides were synthesized on a Milligen DNA synthesizer, purified by reverse-phase HPLC and Q-Sepharose ion-exchange chromatography, dialyzed against deionized water, lyophilized and dissolved in 10 mM HEPES, pH 7.5, 100 mM NaCl. Equimolar amounts of the two strands were mixed and annealed. The final concentration for the double-stranded DNA was 1.6 mM.

The NFAT1-RHR–DNA complex was prepared by direct mixing of NFAT1-RHR and the double-stranded DNA at a 2:1 molar ratio. NFAT1-RHR (4.0 µl of 1.6 mM) was mixed with 2.0 µl double-stranded DNA (1.6 mM), 15 µl deionized water and 6 µl of 5.0 M ammonium acetate.

Crystallization. We obtained two crystal forms, trigonal and orthorhombic, for the NFAT1-RHR–DNA complex. The trigonal crystals were grown by hanging-drop vapor diffusion: 4.5 µl complex was mixed with 4.5 µl well solution (100 mM NaCl, 10 mM $MgCl_2$, 2.5 mM spermine, 6% (v/v) glycerol, 6% (w/v) PEG4000, 50 mM bis-Tris propane, pH 6.3). Needle-like crystals appeared in three weeks, in space group $P3_121$. There is one complex in the asymmetric unit (solvent content 75%). The orthorhombic crystals were grown by a microbatch method. Complex (3.0 µl) was mixed with 1.8–2.2 µl of precipitant solution (100 mM NaCl, 10 mM $MgCl_2$, 2.5 mM spermine, 12–15% (v/v) PEG4000, 50 mM Tris-HCl, pH 8.0). The drops were sealed and kept at 19 °C. Crystals in space group $P2_12_12_1$ appeared in one week and continued to grow for another week, to a maximum size of $0.03 \times 0.03 \times 0.6$ mm^3. There are three complexes in the asymmetric unit (solvent content 50%); DNA stacks parallel to the *b* axis.

X-ray diffraction data collection. All X-ray diffraction data were collected at a temperature of 100 K at the Cornell High Energy Synchrotron Source (CHESS; Ithaca, New York, USA) F-1 beamline, using a Quantum-4 CCD detector (Area Detector Systems). The diffraction data were processed with HKL2000 (ref. 14, HKL Research) and the CCP4 suite[15]. The trigonal crystals yielded data to a resolution of 3.9 Å, whereas the orthorhombic crystals diffracted anisotropically to a highest resolution of 3.1 Å.

Structure determination and refinement. The crystal structures were determined by molecular replacement combined with non-crystallographic symmetry (NCS) averaging and solvent flipping using MOLREP[16] and CNS[17]. For the trigonal form, we located the RHR-N pair by molecular replacement using the 2.7-Å structure of monomeric NFAT1 (ref. 4) as a search model. The resulting difference map showed clear density for DNA, but despite extensive efforts, the two RHR-C domains could not be found either by cross-rotation function, locked rotation or inspection of solvent-flattened or averaged electron density maps. Examination of the crystal packing led to the probable explanation that the two RHR-C domains were disordered in the crystal owing to the lack of crystal contacts to immobilize them.

We therefore turned to the orthorhombic form and carried out a molecular replacement search with the RHR-N pair and DNA from the trigonal crystal as a search model. We located all the three RHR-N pairs and the DNA for the three dimers in the asymmetric unit. To locate the three RHR-C domains we calculated an electron density map with the six RHR-N domains and three DNA fragments, followed by NCS averaging of the RHR-N domains and solvent flipping. The resulting map contained clear density for the RHR-C domains. We positioned the RHR-C pair for the first dimer without ambiguity, incorporated this pair into the model, recalculated electron density maps and improved them by six-fold NCS averaging of the RHR-N domains and solvent flipping. We could then position the other two RHR-C pairs. After rigid-body refinement, both the *R*-factor and R_{free} dropped below 42%.

The structure was improved by iterative rounds of manual rebuilding using O[18] and NCS-restrained refinement using CNS with R_{free} as a monitor. The *R*-factor and R_{free} for the final model are 29.6% and 31.9%, respectively. Refinement statistics are presented in **Table 1**. Figures were produced with MOLSCRIPT[19].

Introduction of mutations into the NFAT1 RHR cDNA. Recombinant NFAT1-RHR[20] (397–694) was expressed in bacteria as hexahistidine-tagged proteins and purified under nondenaturing conditions using Ni-NTA agarose (Qiagen). The SG mutant was constructed by substitution of amino acids 614–621 in the NFAT1-RHR with serine and glycine, using the QuikChange system (Stratagene) for site-directed mutagenesis. Presence of the mutation was confirmed by DNA sequencing.

Electrophoretic mobility shift assay (EMSA). Binding reactions (15 μl) contained 4–128 nM purified recombinant NFAT1-RHR and 10,000 c.p.m. (0.2–0.5 ng) of labeled oligonucleotide in binding buffer (10 mM HEPES, pH 7.5, 125 mM NaCl, 10% (v/v) glycerol, 0.25 mM DTT, 100 μg ml^{-1} poly(dI-dC), 0.8 mg ml^{-1} BSA). After incubation for 20 min at room temperature, free and bound probe were separated using 4% (w/v) PAGE. Radiolabel was quantified using a phosphorimager (Molecular Dynamics) and, for each lane, the radioactivity in the individual NFAT-RHR–DNA complexes was divided by the total radioactivity (monomer + dimer + free probe) to determine the fraction of probe bound in each complex. The probe used in EMSA was: 5′-GATCATCCAGGAATTTCCTAGCTAGCT-3′.

Coordinates. Coordinates have been deposited in the Protein Data Bank (accession code 1PZU).

ACKNOWLEDGMENTS

We acknowledge support from US National Institutes of Health grants to S.C.H. and to A.R. CHESS is supported by the US National Science Foundation. S.C.H is an investigator of the Howard Hughes Medical Institute.

COMPETING INTERESTS STATEMENT

The authors declare that they have no competing financial interests.

Received 6 May; accepted 1 August 2003
Published online at http://www.nature.com/naturestructuralbiology/

1. Crabtree, G.R. & Olson, E.N. NFAT signaling: choreographing the social lives of cells. *Cell* **109** (suppl.), S67–S79 (2002).
2. Rao, A., Luo, C. & Hogan, P.G. Transcription factors of the NFAT family: regulation and function. *Annu. Rev. Immunol.* **15**, 707–747 (1997).
3. Chytil, M. & Verdine, G.L. The Rel family of eukaryotic transcription factors. *Curr. Opin. Struct. Biol.* **6**, 91–100 (1996).
4. Chen, L., Glover, J.N., Hogan, P.G., Rao, A. & Harrison, S.C. Structure of the DNA-binding domains from NFAT, Fos and Jun bound specifically to DNA. *Nature* **392**, 42–48 (1998).
5. Chen, L. Combinatorial gene regulation by eukaryotic transcription factors. *Curr. Opin. Struct. Biol.* **9**, 48–55 (1999).
6. Giffin, M.J. *et al.* Structure of NFAT1 bound as a dimer to the HIV-1 LTR κB element. *Nat. Struct. Biol.* advance online publication, 31 August 2003 (doi:10.1038/nsb981).
7. Ghosh, G., van Duyne, G., Ghosh, S. & Sigler, P.B. Structure of NF-κB p50 homodimer bound to a κB site. *Nature* **373**, 303–310 (1995).
8. Baltimore, D. & Beg, A.A. DNA-binding proteins. A butterfly flutters by. *Nature* **373**, 287–288 (1995).
9. Muller, C.W., Rey, F.A., Sodeoka, M., Verdine, G.L. & Harrison, S.C. Structure of the NF-κB p50 homodimer bound to DNA. *Nature* **373**, 311–317 (1995).
10. Seeman, N.C., Rosenberg, J.M. & Rich, A. Sequence-specific recognition of double helical nucleic acids by proteins. *Proc. Natl. Acad. Sci. USA* **73**, 804–808 (1976).
11. Zhou, P., Sun, L.J., Dotsch, V., Wagner, G. & Verdine, G.L. Solution structure of the core NFATC1/DNA complex. *Cell* **92**, 687–696 (1998).
12. Stroud, J.C., Lopez-Rodriguez, C., Rao, A. & Chen, L. Structure of a TonEBP-DNA complex reveals DNA encircled by a transcription factor. *Nat. Struct. Biol.* **9**, 90–94 (2002).
13. Macian, F. *et al.* Transcriptional mechanisms underlying lymphocyte tolerance. *Cell* **109**, 719–731 (2002).
14. Otwinowski, Z. & Minor, W. Processing of X-ray diffraction data collected in oscillation mode. *Methods Enzymol.* **276**, 307–326 (1997).
15. Collaborative Computational Project, Number 4. The CCP4 suite: programs for protein crystallography. *Acta Crystallogr. D* **50**, 760–763 (1994).
16. Vagin, A. & Teplyakov, A. An approach to multi-copy search in molecular replacement. *Acta Crystallogr. D* **56**, 1622–1624 (2000).
17. Brünger, A.T. *et al.* Crystallography & NMR system: a new software suite for macromolecular structure determination. *Acta Crystallogr. D* **54**, 905–921 (1998).
18. Jones, T.A., Zou, J.Y., Cowan, S.W. & Kjeldgaard, M. Improved methods for the building of protein models in electron-density maps and the location of errors in these models. *Acta Crystallogr. A* **47**, 110–119 (1991).
19. Kraulis, P.J. MOLSCRIPT: a program to produce both detailed and schematic plots of protein structures. *J. Appl. Crystallogr.* **24**, 946–950 (1991).
20. Jain, J., Burgeon, E., Badalian, T.M., Hogan, P.G. & Rao, A. A similar DNA-binding motif in NFAT family proteins and the Rel homology region. *J. Biol. Chem.* **270**, 4138–4145 (1995).